Am J Transl Res 2020;12(7):3311-3328
www.ajtr.org /ISSN:1943-8141/AJTR0107205

Original Article

Baicalin rescues hyperglycemia-induced neural tube defects via targeting on retinoic acid signaling

Guang Wang[1*], Jia-Qi Lu[2*], Yong Ding[2*], Tonghua Zhang[1], Jin-Huan Song[1], Denglu Long[1], Jianxin Liang[1], Xin Cheng[1], Zhenpeng Si[3], Guolong Qi[4], Xiaohua Jiang[5], Xuesong Yang[1,6]

[1]Division of Histology and Embryology, International Joint Laboratory for Embryonic Development & Prenatal Medicine, Medical College, Jinan University, Guangzhou 510632, China; [2]Department of Ophthalmology, The First Affiliated Hospital of Jinan University, Guangzhou 510632, China; [3]Department of Pediatrics and Neonatology, Institute of Fetal-Preterm Labor Medicine, The First Affiliated Hospital, Jinan University, Guangzhou 510630, China; [4]Division of Medical Information, Medical College, Jinan University, Guangzhou 510632, China; [5]Key Laboratory for Regenerative Medicine of The Ministry of Education of China, School of Biomedical Sciences, Faculty of Medicine, The Chinese University of Hong Kong, Hong Kong SAR, China; [6]Key Laboratory for Regenerative Medicine of The Ministry of Education, Jinan University, Guangzhou 510632, China. [*]Equal contributors.

Received December 31, 2019; Accepted May 29, 2020; Epub July 15, 2020; Published July 30, 2020

Abstract: We, in this study, studied whether or not antioxidant activities of Baicalin could reduce the incidence of neural tube defects (NTDs) in the presence of hyperglycemia. Using early chick embryos, we demonstrated that Baicalin at 6 μM dramatically reduced NTDs rate and impaired neurogenesis in E4.5-day and HH10 chick embryo neural tubes induced by high glucose (HG). Likewise, immunofluorescent staining showed that Baicalin mitigated the HG-induced regression of Pax7 expression in neural tubes of both HH10 and E4.5-day chick embryos. Additionally, PHIS3 immunofluorescent staining in neural tubes of both HH10 and E4.5-day chick embryos manifested that cell proliferation inhibited by HG was significantly reversed by the administration of Baicalin, and similar result could also be observed in neurosphere assay *in vitro*. c-Caspase3 or γH2AX immunofluorescent staining and quantitative PCR showed that Baicalin administration alleviated HG-induced cell apoptosis and DNA damage. Bioinformatics results indicated that retinoic acid (RA) was likely to be the signaling pathway that Baicalin targeted on, and this was confirmed by whole-mount RALDH2 *in situ* hybridization and quantitative PCR of HH10 chick embryos in the absence/presence of Baicalin. In addition, blocking RA with an inhibitor abolished Baicalin's protective role in HG-induced NTDs, suppression of neurogenesis and cell proliferation, and induction of apoptosis, which further verified the centrality of RA in the process of Baicalin confronting HG-induced abnormal neurodevelopment.

Keywords: Baicalin, HG, neural tube defects, neural differentiation, retinoic acid

Introduction

The neural tube is the rudiment of the central nervous system, which can be spatially divided into cranial and trunk regions. The cranial region gives rise to the brain, whereas the trunk region develops into the spinal cord in adulthood. During neurulation, neural tube formation refers to a dynamic process, which undergoes the elevation and bend of neural plate into a fluid-filled tube in dorsal midline eventually. These processes rely on pattern determining genes to be accurately expressed in dorsal and ventral regions of neural tubes [1]. Normal neurulation is governed by a variety of cellular events, such as cell proliferation, apoptosis, cytoskeleton establishment and cell viability, etc. [2], which are precisely regulated and controlled by a variety of signaling molecules, such as FGF, Wnt, Hh and TGF-beta [3]. Neural tube defects (NTDs) are defined as improperly developed neural tubes characterized by the open neural tubes in the brain or spinal cord at birth. Pathologic causes of NTDs could be multifactorial, with involvement of both genetic and environmental factors [4, 5]. In fact, NTDs still remain as one of the commonest categories of congenital birth defects worldwide even after

the discovery of preventive effects of folic acid [6].

Nervous system as one of the earliest two developed systems during embryogenesis, is extremely sensitive to the changes of external environment, such as maternal hyperglycemia derived from type II diabetes of pregnant women or gestational diabetes mellitus (GDM). GDM presents with high maternal blood glucose levels at the early stage of pregnancy, due to glucose intolerance. Of note, it has been reported that the incidence of congenital disorders is 2-5 times higher in diabetic pregnancy than that in non-diabetic pregnancy [7]. Our previous studies clearly indicated that high glucose (HG) levels increased the risk of avian embryonic malformation through a variety of biological mechanisms [8-10]. In addition, Liu et al. demonstrated that diabetes could lead to apoptosis of neural progenitor cells that in turn induced NTDs in embryos [11]. However, effective drugs are yet to be developed to prevent defective embryonic development under the condition of maternal diabetes mellitus.

Baicalin is a flavone glycoside (the glucuronide of baicalein), which is generated from the combination of both glucuronic acid and baicalein. Baicalein is a type of flavone existing in the roots of *Scutellaria lateriflora* and *Scutellaria baicalensis*, while the roots of *Scutellaria baicalensis* have been employed to calm fetuses in pregnant women in Chinese medicine [12, 13]. Baicalin is actually predominantly used as an herbal supplement in Asian countries due to its broad scope of health benefits, such as anti-neuroinflammation [14], anti-cancer [15], anti-anxiety [16], and increase of lung capability [17] and fertility [18]. In terms of biological mechanism, Baicalin is essentially considered to suppress the formation of oxidative stress [19]. Qi *et al*. reported that Baicalin could maintain normal development of mouse embryos through inhibiting cell apoptosis and HSP70 expression, and activating DNA methylation [20]. Our previous study indicated that Baicalin administration attenuated HG-induced malformation of cardiovascular system [21]. However, whether or not Baicalin could prevent or rescue the neural tube malformation under HG at an early developmental stage still remains elusive. Thus, the present study focuses on the beneficial or protective effects of Baicalin and its corresponding mechanism on confronting HG-induced damage to early neural development, using early chick embryo as an experimental model that have been proven effective in our previous studies [9, 22].

Materials and methods

Avian embryos and treatment

Fertilized chick eggs were obtained from the Avian Farm of the South China Agriculture University. The eggs were incubated until the chick embryos reached the desired developmental HH stage [23] in a humidified incubator (Yiheng Instrument, Shanghai, China) at 38°C and 70% humidity. For the later stage chick embryos, 1.5-day pre-incubated chick embryos were exposed to either different concentrations of Baicalin (Santa Cruz Biotechnology, Dallas, TX, USA) or same amount (approximately 200 μL) of 0.9% sterile saline through careful injection into windowed eggs *in vivo* (**Figure 1A**). For early gastrula embryos, HH0 [23] chick embryos were prepared and incubated with saline, 6 μM Baicalin, 1 μM retinoic acid (Sigma-Aldrich, R2625) [24], 10 μM AGN (Sigma-Aldrich, SML2034) [25] or/and 50 mM glucose (Sigma, USA), using early chick culture (EC culture) (**Figure 2A**) [8-10, 26].

Histology and photography

The treated embryos were further incubated and harvested at the desired times from the incubation at 38°C based on the experimental requirements. All of the embryos were photographed using a stereomicroscope (Olympus MVX10, Japan) before being fixed with 4% paraformaldehyde for morphological analysis and gene expression determination. For the histological analysis, the E4.5-day embryos were dehydrated, embedded in paraffin wax and serially sectioned at 5 μm using a microtome (Leica RM2126RT, Germany). The sections were dewaxed in xylene, rehydrated and stained with either hematoxylin and eosin dye or immunofluorescent staining, and photographed using a fluorescent microscope (Olympus IX50) with the NIS-Elements F3.2 software package.

Immunofluorescent staining

Chick embryos were harvested after a given time incubation and fixed in 4% PFA overnight at 4°C. Immunofluorescent staining was performed on either whole-mount embryos or tran-

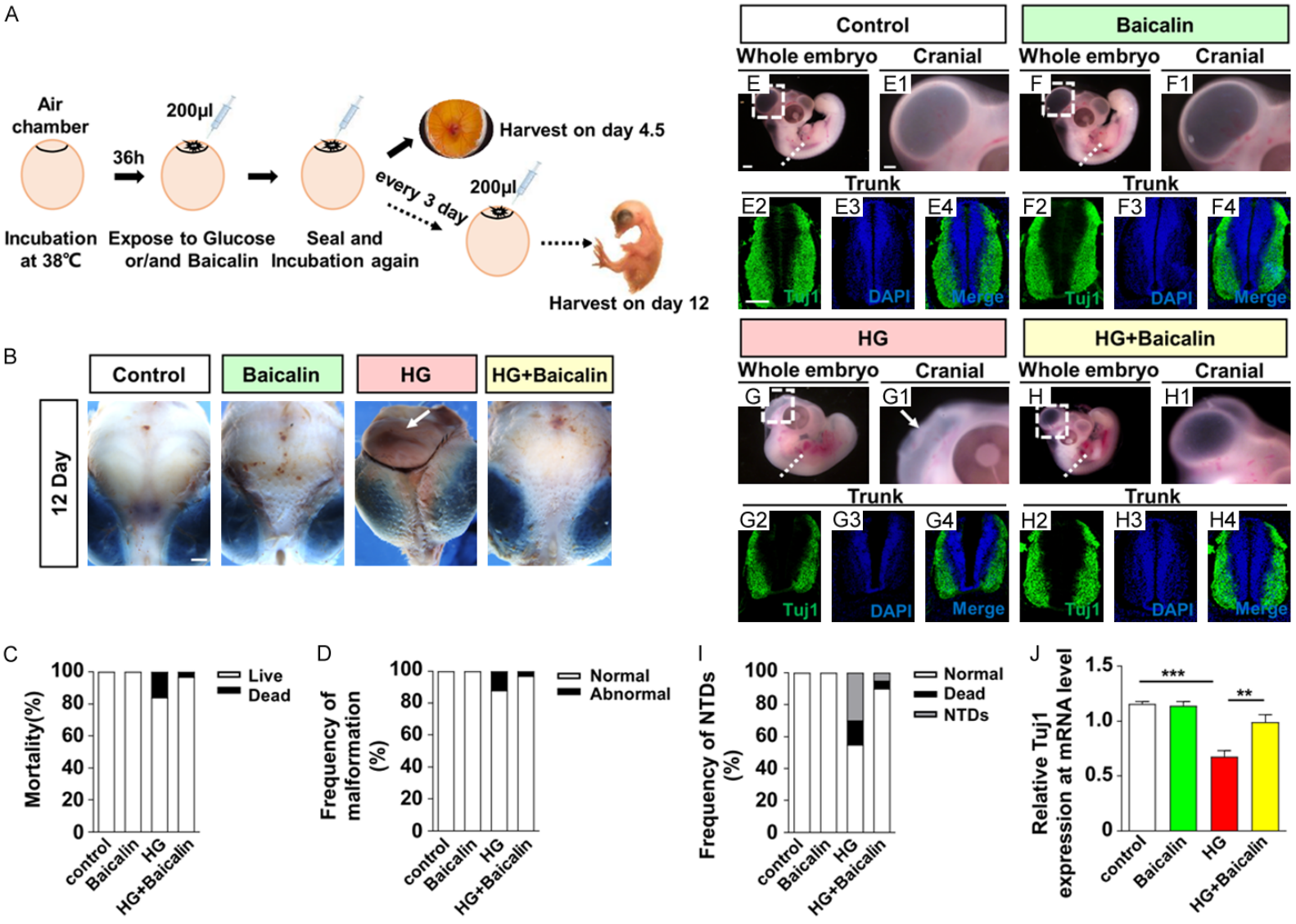

Figure 1. The assessment of cranial neural tube development of chick embryos exposed to HG in the absence/presence of Baicalin. (A) The sketch illustrating the timing that glucose or/and Baicalin was applied to developing chick embryos through air chamber of fertilized eggs *in vivo*, and the treated-embryos were harvested (see material and method section for details). (B) The representative bright-field images of 12-day chick embryos' head from control, 6 μM Baicalin, 50 mM HG, 50 mM HG + 6 μM Baicalin group respectively. (C, D) Bar charts showing the comparisons of the mortality (C) and malformation (D) of 12-day chick embryos among control, Baicalin, HG, HG + Baicalin groups. (E-H) The representative bright-field images of E4.5-day chick embryos' cranial bones from control (E), Baicalin (F), HG (G), HG + Baicalin (H) group respectively. (E1-H1) The high magnification images from cephalic regions of chick embryos indicated by dotted squares in (E-H) respec-

tively. (E2-4, F2-4, G2-4, H2-4) The Tuj1 immunofluorescent, DAPI and merge images on the transverse sections at the level indicated by dotted lines in (E-H) from control (E2-4), Baicalin (F2-4), HG (G2-4), HG + Baicalin (H2-4) group respectively. (I, J) Bar charts showing the comparisons of the NTDs frequency (I) and relative Tuj1 expression at mRNA level (J) revealed by quantative PCR in E4.5-day chick embryos among control, Baicalin, HG, HG + Baicalin groups. For (B-D), n=25 in each group, for (E-I), n=20 in each group, for (J), n>3 in each group, relative to GAPDH mRNA level, **P<0.01, ***P<0.001. Data were presented as mean ± SE. Statistical significances were assessed by one-way ANOVA and Turkey's multiple comparisons test. Scale bars =1 mm in (B); 1 mm in (E-H); 500 μm in (E1-H1); 100 μm in (E2-4, F2-4, G2-4, H2-4).

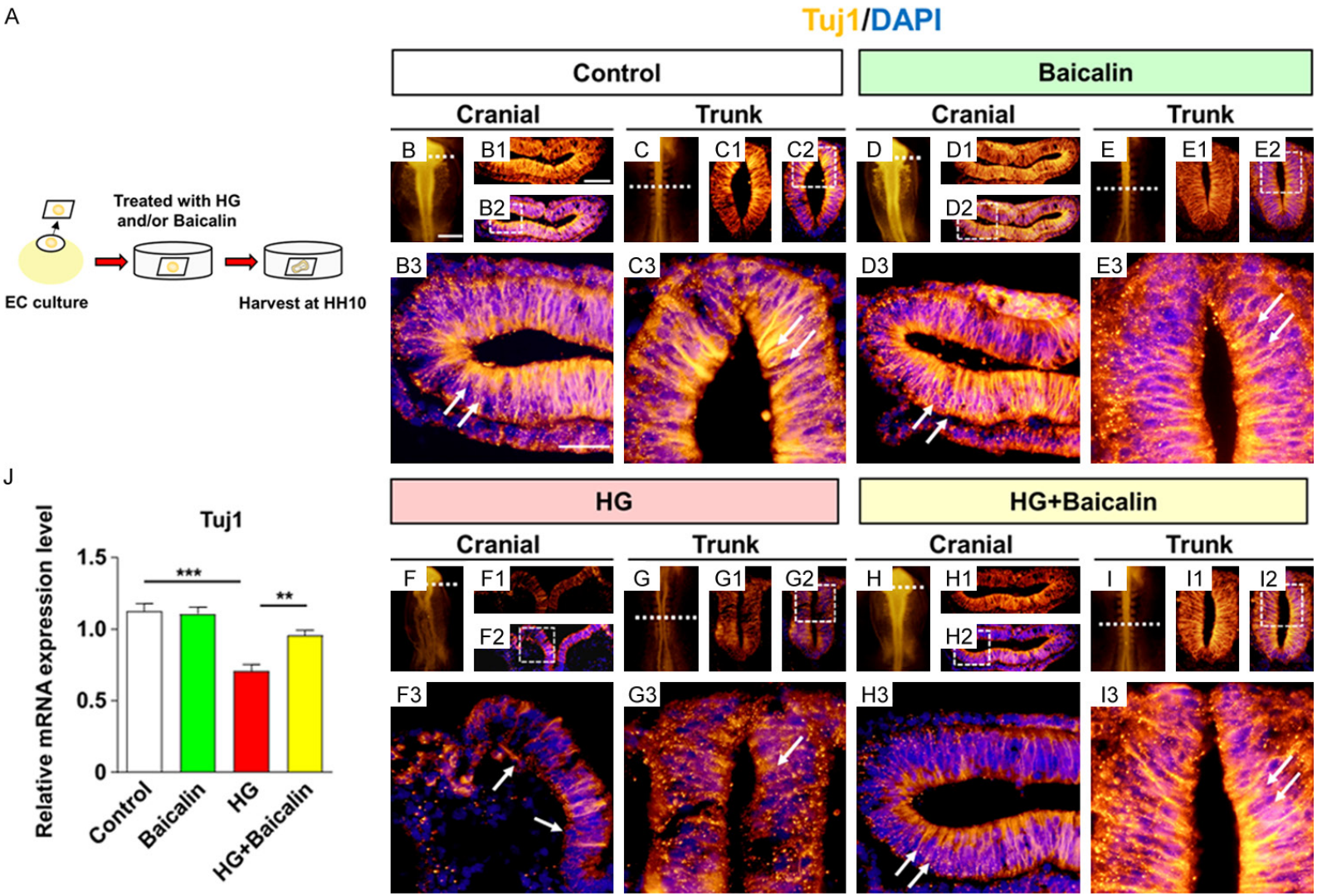

Figure 2. The assessment of Tuj1-labelled neural differentiation of gastrula chick embryos in the absence/presence of HG and Baicalin. (A) The sketches illustrating the gastrula chick embryo incubation with EC culture. (B-I) The representative images of Tuj1 immunofluorescent HH10 chick embryos from control (B, C), 6 μM Baicalin (D, E), 50 mM HG (F, G), 50 mM HG + 6 μM Baicalin (H, I) group respectively. Of them, the images were divided into cranial and trunk regions. (B1-I1, B2-I2) The transverse sections at the levels indicated by dotted lines in (B-H) respectively (B1-I1), and counterstained with DAPI (B2-I2). (B3-I3) The high magnification images from the sites indicated by dotted squares in (B2-I2) respectively. (J) Bar chart showing the quantative PCR data about the Tuj1 expression at mRNA level in HH10 chick embryos among control, Baicalin, HG, HG + Baicalin groups. For (B-I), n=6 in each group, for (J), n>3 in each group, relative to GAPDH mRNA level, **P<0.01, ***P<0.001. Data were presented as mean ± SE. Statistical significances were assessed by one-way ANOVA and Turkey's multiple comparisons test. Scale bars =300 μm in (B-I); 100 μm in (B1-I1, B2-I2); 50 μm in (B3-I3).

sverse sections using the following antibodies: Tuj1 (1:200, Neuromics, USA), Pax7 (1:200, DSHB, USA), phospho-histone3 (PHIS3; 1:200, Santa Cruz, USA) PCNA (1:400, DSHB, USA), cleaved-caspase3 (c-Caspase3; 1:200, Cell Signaling Technology, USA), γH2AX (1:200, DSHB, USA). Briefly, the fixed embryos or transverse sections were then incubated with these primary antibodies at 4°C overnight on a shaker. Following by extensive washing, the embryos were incubated with an anti-rabbit IgG conjugated to Alexa Fluor 488 or Alexa Fluor 555 overnight at 4°C on a rocker. All the samples were later counterstained with DAPI (1:1000, Invitrogen, USA) at room temperature for 1 hour.

In situ hybridization

Whole-mount *in situ* hybridization of chick embryos was performed according to a standard *in situ* hybridization protocol [27]. Digoxigenin-labeled probes were synthesized against RALDH2 [21], RARβ [21] and SHH [10]. The stained whole-mount chick embryos were photographed by a stereomicroscope (Olympus MVX10, Tokyo, Japan) and then prepared for cryosectioning on a cryostat microtome with 16 μm thickness (Leica CM1900).

RNA isolation and quantitative PCR

Total RNA was isolated from chick embryos using a Trizol kit (Invitrogen, USA) according to the manufacturer's instructions. First-strand cDNA was synthesized to a final volume of 20 μl using iScriptTM cDNA Synthesis Kit (BIO-RAD, USA). Following reverse transcription, PCR amplification of the cDNA was performed as described previously [28, 29]. SYBR® Green qPCR assays were then performed using a PrimeScriptTM RT reagent kit (Takara, Japan). All specific primers used are described in Supplementary Table 1. Reverse transcription and amplification reactions were performed in Bio-Rad S1000TM (Bio-Rad, USA) and ABI 7000 thermal cyclers, respectively. The housekeeping gene GAPDH was run in parallel to confirm that equal amounts of RNA were used in each reaction. The expression of the genes was normalized to GAPDH, and the expression level of target genes was done based on the $2^{-\Delta\Delta Ct}$ method. At least three replicates were done for each sample.

Enzyme-linked immunosorbent assay (ELISA)

RA (Jiangsu Meibiao Biological Technology Co. Ltd., Jiangsu, China) or homocysteine (Cloud-Clone Corp, Houston, USA) levels were detected in chick embryos using ELISA kits according to the manufacturer's instructions. The levels of RA or homocysteine were calculated based on their standard curves created by different concentrations against absorbance, respectively.

Primary culture of neural stem cells

The methods of neural stem cell isolation and incubation were performed as previously described [30]. In brief, the hippocampi were removed from the brain of postnatal day 1 mice and transferred to a 35-mm plate containing PBS with 2% D-glucose on ice. The re-suspended hippocampi in NSC medium were triturated with a fire-polished glass pipet (Brainbits, IL, USA). The supernatant containing single cells were plated into a fresh tube, centrifuged, and re-suspended in NSC medium, and seeded at a density of 2×10^6 cells per 10 ml. The cells were cultured in a humidified incubator with 5% CO_2 at 37°C in T-25 cm flask with NSC medium, which contains DMEM/F-12 (Gibco, China) supplemented with 2% B27 (Gibco, USA), 20 ng/ml of rmEGF (Gibco, CA, USA), 20 ng/ml of rmbFGF (Gibco, USA) and exposed to HG (50 mM) and/or Baicalin (6 μM) with PBS acting as a control.

After a 7-day incubation, the neurospheres were photographed using inverted microscope (Nikon Eclipse Ti-U, Tokyo, Japan) that was linked to the NIS Elements F3.2 software.

Bioinformatics analysis

GO (Gene Ontology) enrichment analysis and KEGG (Kyoto Encyclopedia of Genes and Genomes) pathway enrichment analysis were performed using the DAVID (Database for Annotation, Visualization, and Integrated Discovery) tools [31].

Data analysis

The various markers' positive cell rates and relative mRNA expressions in the different experimental samples were analyzed using the Image Pro-Plus 5.0 software [32]. Statistical analysis was performed using a SPSS 13.0 statistical package program for Windows. The data were presented as mean ± SE. Statistical significance was assessed by one-way ANOVA and Turkey's multiple comparisons test. $P<0.05$ was considered to be statistically significant.

Results

Baicalin administration efficiently reverses HG-induced malformation of early nervous system in chick embryos

First, to determine the optimal concentration of Baicalin, we evaluated the development of gastrula chick embryos exposed to 50 mM HG with different concentrations of Baicalin (Supplementary Figure 1). The combinational application of HG and Baicalin administration at early stage of chick embryos *in vivo* showed that 6 μM Baicalin most significantly inhibited the percentage of HG-induced NTDs as shown with white arrows (Supplementary Figure 1A, 1B). Additionally, 6 μM Baicalin administration mitigated the suppressive effects of HG on embryo development (Supplementary Figure 1C-E). Next, we exposed the chick embryo to HG or/and Baicalin and harvested them on day 12 and day 4.5 (**Figure 1A**). Baicalin itself did not affect embryo development, but it reduced the incidence of HG-induced mortality and malformation (indicated by arrow, **Figure 1B**) of E12-day chick embryo including cranial NTDs (Mortality rates: 0% in control and Baicalin, 16% in HG, 4% in HG + Baicalin; malformation rates: 0% in control and Baicalin, 20% in HG, 4% in HG + Baicalin. **Figure 1C**, **1D**). In particular, the incidence of NTDs of E4.5-chick embryos increased in the presence of HG, but decreased when Baicalin was jointly applied (Mortality rates: 0% in control and Baicalin, 15% in HG, 5% in HG + Baicalin; NTDs rates: 0% in control and Baicalin, 30% in HG, 5% in HG + Baicalin. **Figure 1E-I**, **1E1-H1**). The expression level of Tuj1 (neuronal differentiation marker) was significantly reduced in HG-treated embryos at the corresponding trunk level (indicated by dotted lines) as illustrated by immunofluorescent staining. Interestingly, the suppressive effect on Tuj1 by HG was mostly reversed by Baicalin (**Figure 1E2-H2**, **1E3-H3**, **1E4-H4**). In addition, quantitative PCR data also showed that HG-inhibited Tuj1 expression was significantly alleviated by addition of 6 μM Baicalin (**Figure 1J**).

Baicalin alleviates HG-induced neural malformation at early neurulation stage partly through dorsal-ventral pattering

HG has been shown to play negative effects on early embryo development [33]. To investigate at which stage Baicalin plays confrontational role in rescuing HG-induced suppression in neurogenesis, we implemented the similar mentioned-above experiments at gastrula chick embryos using EC culture (**Figure 2A**). First, we observed that Tuj1 expression in both cranial and trunk levels (indicated by arrows) of HH10 chick embryos was suppressed by HG, but dramatically recovered after the administration of Baicalin (**Figure 2B-I**, **2B1-I1**, **2B2-I2**, **2B3-I3**). Meanwhile, quantitative PCR analysis revealed that Tuj1 expression at mRNA level was also significantly reversed by Baicalin compared with the HG group (**Figure 2J**). Second, we determined Pax7 expression in the same HH10 and E4.5-day chick embryos since Pax7 is regulated by BMP4 pathway and is expressed in dorsal neural tube [1]. The results manifested that Baicalin administration effectively reversed the reduction of Pax7 expression at mRNA level from HH10 and E4.5-day chick embryos treated with HG (Percentage of Pax7 positive cells in HH10: 33.40 ± 1.20% in control, 34.46 ± 1.31% in Baicalin, 18.20 ± 1.39% in HG, 30.78 ± 0.71% in HG + Baicalin; percentage of Pax7 positive cells in E4.5-Day: 36.92 ± 1.15% in control, 35.78 ± 1.87% in Baicalin, 19.06 ± 0.76% in HG, 32.84 ± 0.91% in HG + Baicalin. **Figure 3A-K**), implying that the HG-induced NTDs could be considerably relieved by admin-

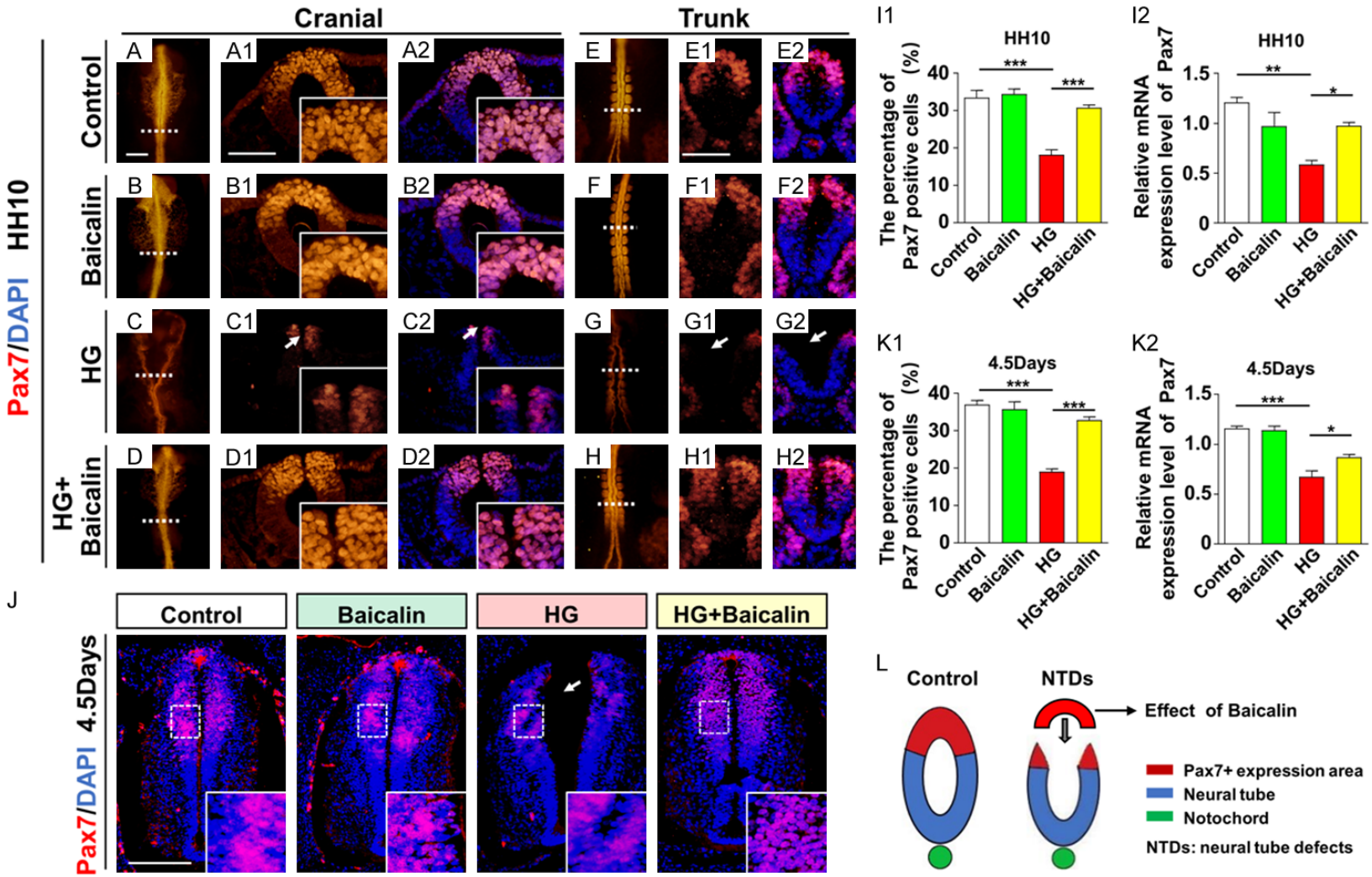

Figure 3. The assessment of Pax7-labelled neural tube development during embryonic neurulation in the absence/presence of HG and Baicalin. (A-H) The representative Pax7 immunofluorescent staining of HH10 chick embryos from control (A, E), 6 μM Baicalin (B, F), 50 mM HG (C, G), 50 mM HG + 6 μM Baicalin (D, H) group respectively. Of them, the images were divided into cranial (A-D) and trunk (E-H) regions. (A1-H1, A2-H2) The transverse sections at the levels indicated by dotted lines in (A-H) respectively (A1-H1), and counterstained with DAPI (A2-H2). (J) Pax7 immunofluorescent staining was performed on the transverse sections of E4.5-day chick embryonic neural tubes from control, Baicalin, HG, HG + Baicalin groups. Note: the high magnification images were shown in the lower right corner accordingly. (I1, I2, K1, K2) Bar charts showing the comparisons of the Pax7 positive cell percentages in the total DAPI-labelled cells of neural tubes (I1, K1) and

relative Pax7 expression at mRNA level (I2, K2) revealed by quantitative PCR in HH10 (I1, I2) or E4.5-day (K1, K2) chick embryos among control, Baicalin, HG, HG + Baicalin groups. (L) The sketches illustrating the normal neural tube and NTDs. For (A-H, J, I1, K1), n=5 in each group, for (I2, K2), n>3 in each group, relative to GAPDH mRNA level, *P<0.05, **P<0.01, ***P<0.001. Data were presented as mean ± SE. Statistical significances were assessed by one-way ANOVA and Turkey's multiple comparisons test. Scale bars =300 μm in (A-H); 100 μm in (A1-H1), 50 μm in (A2-H2); 100 μm in (J).

istration of Baicalin (**Figure 3L**). In contrast, the rescue effects of Baicalin on SHH expression was not statistically significant in the ventral side of neural tube (Supplementary Figure 2).

Re-balance between cell proliferation and apoptosis contributes to the protective role of Baicalin

To understand the cellular mechanisms underlying the protective effect of Baicalin, we determined the expression levels of PHIS3 and PCNA (cell proliferation) and c-Caspase3 (apoptosis) in the neural tubes of HH10 and E4.5-chick embryos under HG in the absence/presence of Baicalin. Immunofluorescent staining of PHIS3 (**Figure 4A**) and PCNA (**Figure 4B**) showed that HG inhibited the expressions of PHIS3 and PCNA in neural tubes of HH10 and E4.5-day chick embryos, but the inhibitory effects were significantly reversed by addition of Baicalin (Number of PHIS3 positive cells: 14.60 ± 0.60 in control, 13.60 ± 0.51 in Baicalin, 8.20 ± 0.86 in HG, 12.60 ± 0.51 in HG + Baicalin; percentage of PCNA positive cells: 58.62 ± 1.15% in control, 56.58 ± 0.57% in Baicalin, 47.23 ± 0.73% in HG, 54.68 ± 0.67% in HG + Baicalin. **Figure 4C**, **4D**). On the contrary, both the immunofluorescent staining and quantitative PCR data showed that HG significantly increased the expression of γH2AX (marker for DNA damage) and c-Caspase3 (apoptosis) in neural tubes of HH10 chick embryos; however, both HG-induced DNA damage and apoptosis dropped back to normal in the presence of Baicalin (Number of c-Caspase3 positive cells: 1.75 ± 0.25 in control, 1.5 ± 0.29 in Baicalin, 4.75 ± 0.48 in HG, 2.00 ± 0.41 in HG + Baicalin; number of γH2AX positive cells: 6.40 ± 0.51 in control, 7.60 ± 0.51 in Baicalin, 14.80 ± 0.73 in HG, 9.20 ± 0.86 in HG + Baicalin. **Figure 5A-F**). Moreover, the expression level of P53 and concentration of homocysteine were also increased in the presence of HG, whereas a partial recovery was observed after Baicalin treatment (Concentration of homocysteine: 8.65 ± 0.01 μg/ml in control, 9.36 ± 0.20 μg/ml in Baicalin, 19.23 ± 0.23 μg/ml in HG, 13.87 ± 0.12 μg/ml in HG + Baicalin. **Figure 5G**, **5H**). All of these results imply that Baicalin promotes proliferation and alleviates HG-induced cell apoptosis in early developing embryo. As a first step to investigate the direct role of Baicalin in neural progenitor cell function, we isolated primary neural precursors from neonatal mice. Using neurosphere *in vitro* culture, freshly isolated neural precursors were exposed to HG in the presence or absence of Baicalin. In striking consistency with the *in vivo* data, we observed that Baicalin administration rescued the suppressive effects of HG on neurosphere formation (% NS-forming cells: 100.00 ± 4.64 in control, 99.56 ± 2.44 in Baicalin, 78.11 ± 0.88 in HG, 94.96 ± 1.46 in HG + Baicalin; diameter of NS: 237.40 ± 11.01 μm in control, 226.80 ± 2.30 μm in Baicalin, 185.50 ± 2.08 μm in HG, 237.40 ± 7.78 μm in HG + Baicalin; number of NS: 23.40 ± 0.51 in control, 22.00 ± 0.84 in Baicalin, 9.80 ± 0.86 in HG, 20.40 ± 1.03 in HG + Baicalin. **Figure 4E-H**), indicating that the restoration of balance between proliferation and apoptosis in neural precursors contributes to the protective effect of Baicalin during early embryo development under HG.

RA signaling mediates the protective role of Baicalin

Using the DAVID tools, GO enrichment analysis and KEGG pathway enrichment analysis indicated that the genes in this study were indirectly involved in cell cycles, apoptosis, neural differentiation and cell fate commitment during neural tube development, and all the targeted genes could be regulated by RA signaling (**Figure 6A**). ELISA assays indicated that the content of RA in HH10 chick embryos decreased in the presence of HG, and reversed by Baicalin administration (Concentration of RA: 2.73 ± 0.08 ng/ml in control, 2.58 ± 0.09 ng/ml in Baicalin, 1.60 ± 0.08 ng/ml in HG, 1.97 ± 0.05 ng/ml in HG + Baicalin. **Figure 6B**). Furthermore, both quantitative PCR and *in situ* hybridization data showed that the expression of RALDH2 (retinal dehydrogenase 2), a gene encoding crucial enzyme for generating RA, was inhibited by

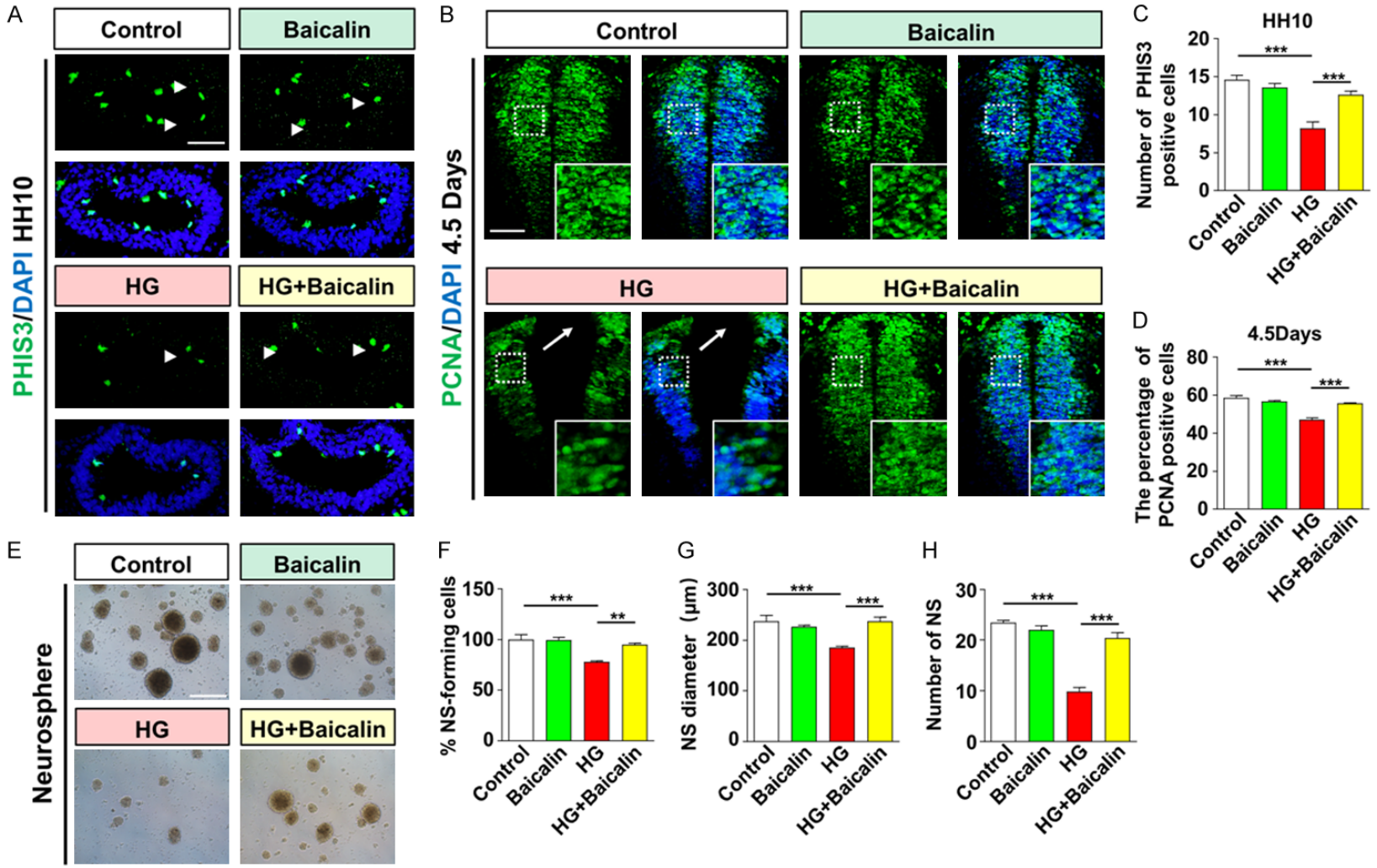

Figure 4. The assessment of neural progenitor cell proliferation in the absence/presence of HG and Baicalin. (A, B) PHIS3 (A) or PCNA (B) immunofluorescent staining was performed on the transverse sections of HH10 (A) or E4.5-day (B) chick embryonic neural tubes from control, 6 μM Baicalin, 50 mM HG, 50 mM HG + 6 μM Baicalin group respectively, and counterstained with DAPI. The high magnification images are in the lower right corner accordingly. (C, D) Bar charts showing the comparisons of the PHIS3 (C) or PCNA (D) positive cell percentages in the total DAPI-labelled cells of neural tubes among control, Baicalin, HG, HG + Baicalin groups. (E) The representative bright-field images of *in vitro* neurospheres (NS) incubated with PBS (control), Baicalin, HG, HG + Baicalin. (F-H) Bar charts showing the comparisons of the neurosphere-forming cell percentages (F), neurosphere diameters (μm) (G), and neurosphere numbers (H) among control, Baicalin, HG, HG + Baicalin groups. For (A-D, F-H), n=5 in each group, **P<0.01, ***P<0.001. Data were presented as mean ± SE. Statistical significances were assessed by one-way ANOVA and Turkey's multiple comparisons test. Scale bars =100 μm in (A, B); 100 μm in (E).

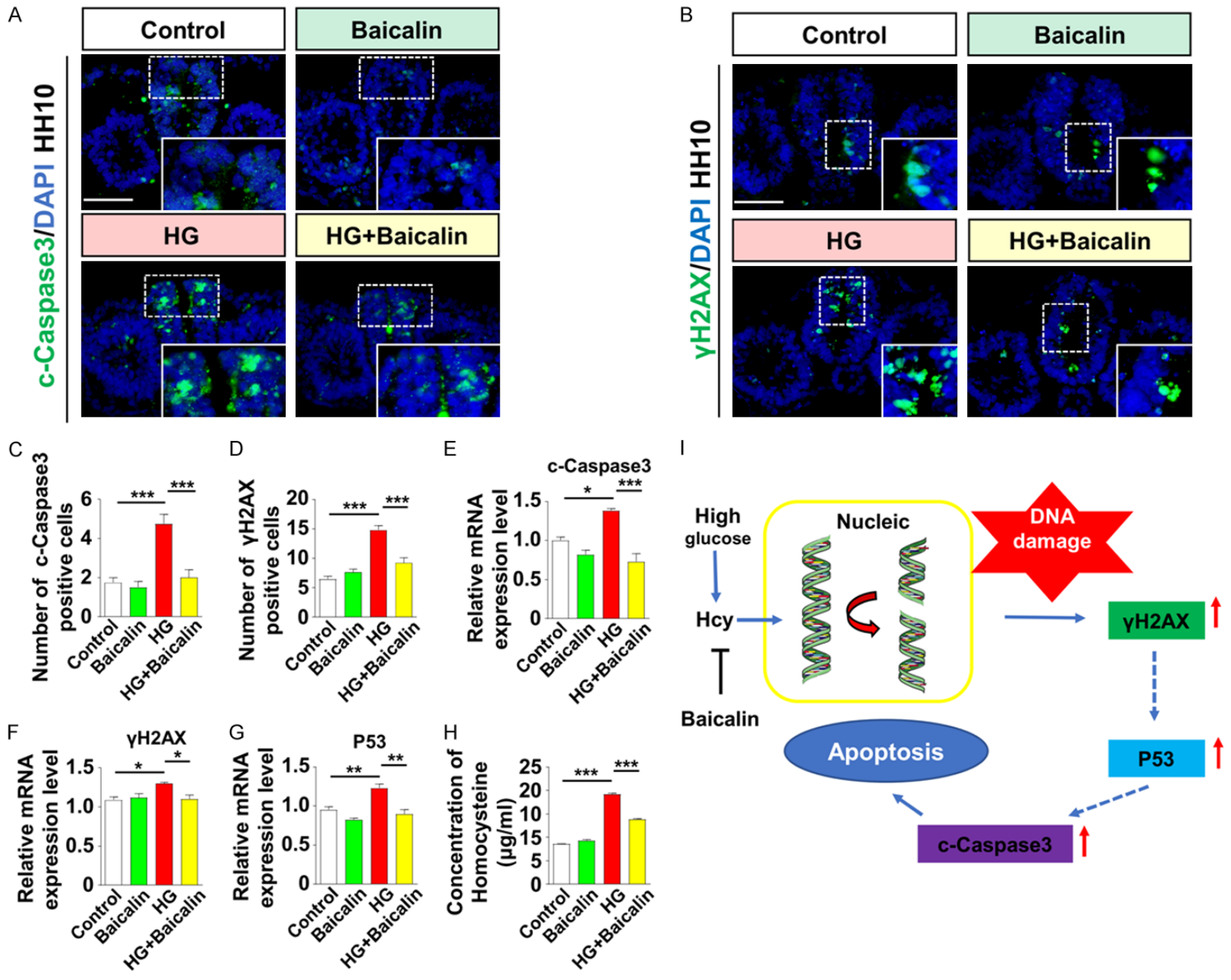
A
Control
Baicalin
HG
HG+Baicalin
c-Caspase3/DAPI HH10
B
Control
Baicalin
HG
HG+Baicalin
γH2AX/DAPI HH10
C
Number of c-Caspase3 positive cells
D
Number of γH2AX positive cells
E
c-Caspase3
Relative mRNA expression level
F
γH2AX
Relative mRNA expression level
G
P53
Relative mRNA expression level
H
Concentration of Homocysteine (μg/ml)
Control
Baicalin
HG
HG+Baicalin
I
High glucose
Hcy
Baicalin
Nucleic
DNA damage
γH2AX
P53
c-Caspase3
Apoptosis

Figure 5. The assessment of DNA damage and apoptosis in neural progenitor cells of neural tubes in the absence/presence of HG and Baicalin. (A, B) c-Caspase3 (A) or γH2AX (B) immunofluorescent staining was performed and/or counterstained with DAPI on the transverse sections of HH10 chick embryonic neural tubes from control, 6 μM Baicalin, 50 mM HG, 50 mM HG + 6 μM Baicalin group respectively. The high magnification images are from the sites indicated by dotted squares accordingly. (C, D) Bar charts showing the comparisons of the c-Caspase3 (C) or γH2AX (D) positive cell percentages in the total DAPI-labelled cells of neural tubes among control, Baicalin, HG, HG + Baicalin groups. (E-H) Bar charts showing the mRNA expression (quantative PCR) of c-Caspase3 (E), γH2AX (F), P53 (G), and the concentration of Homocysteine (Hcy) (H) in HH10 chick embryo neural tubes among control, Baicalin, HG, HG + Baicalin groups (The concentration of homocysteine were determined by Elisa). (I) The sketches illustrating the possible pathway of DNA damage-induced cell apoptosis under HG through Homocysteine and Baicalin could suppressed it. For (A, B, D), n=5 in each group, for (C), n=4 in each group, for (H), n=3 in each group, for (E-G), n>3 in each group, relative to GAPDH mRNA level, *P<0.05, **P<0.01, ***P<0.001. Data were presented as mean ± SE. Statistical significances were assessed by one-way ANOVA and Turkey's multiple comparisons test. Scale bars =100 μm in (A, B).

HG and significantly rescued by Baicalin administration (**Figure 6C**, **6E-H**). In contrast, no significant change was observed with a few cytochrome P450 family 26 subfamily (the genes involved in metabolic inactivation of RA) except for CYP3A4 (**Figure 6D**, **6I1-I3**). Meanwhile, we also detected the expressions of RARα and RARβ (ligand-inducible transcriptional regulators) at mRNA level. The results showed that the mRNA expression of RARα instead of RARβ was consistent with the one of RA signaling (Supplementary Figure 3).

Then, we detected whether or not the HG-induced neural tube malformation could be rescued by RA. We exposed the chick embryos to HG or/and RA, and found that RA could rescue the mortality, NTDs and neurogenesis induced by HG (NTDs rates: 0% in control, 36% in HG, 12% in HG + RA, 8% in HG + Baicalin, 32% in HG + Baicalin + AGN; mortality rates: 0% in control, 32% in HG, 8% in HG + RA, 4% in HG + Baicalin, 40% in HG + Baicalin + AGN. **Figure 7E**) as indicated by the immunofluorescent staining of Pax7 and Tuj1 (Percentage of PAX7 positive cells: 22.80 ± 1.00% in control, 14.22 ± 1.25% in HG, 20.20 ± 0.86% in HG + RA, 20.60 ± 0.68% in HG + Baicalin, 12.12 ± 0.71% in HG + Baicalin + AGN. **Figure 7A**, **7B**, **7F**). In addition, RA significantly increased PHIS3 and decreased c-Caspase3 positive cells in chick embryos exposed to HG (Number of PHIS3 positive cells: 11.80 ± 0.80 in control, 5.80 ± 0.86 in HG, 11.00 ± 0.63 in HG + RA, 11.40 ± 0.60 in HG + Baicalin, 7.00 ± 0.71 in HG + Baicalin + AGN; number of c-Caspase3 positive cells: 2.33 ± 0.42 in control, 5.16 ± 0.48 in HG, 2.50 ± 0.22 in HG + RA, 2.67 ± 0.33 in HG + Baicalin, 5.50 ± 0.43 in HG + Baicalin + AGN. **Figure 7C**, **7D**, **7G**, **7H**). In order to further verify the involvement of RA signaling in the protective effects of Baicalin, we carried out the similar experiments as mentioned-above when RA signaling was blocked with AGN (an potent RA receptor antagonist) (**Figure 7**). The assessment of embryonic neurulation using immunofluorescent staining of Pax7 and Tuj1 showed that blockage of RA signaling completely abolished Baicalin's protective effects on HG-induced morality, NTDs and defect in neurogenesis (**Figure 7A**, **7B**, **7E**, **7F**). Besides, the suppression of retinoid acid signaling also abrogated the increase of proliferation and decrease of apoptosis by Baicalin treatment under HG condition (**Figure 7C**, **7D**, **7H**). Altogether, these results indicate the indispensable role of RA signaling underlying Baicalin's protective effects during neural tube formation (**Figure 7I**).

Discussion

The vast majority of the experiments in the present study were implemented using chick embryos as the embryo model. The advantage of this model is that chick embryos can grow outside of uterus, so that there is a huge advantage for using chick embryos to precisely observe the effect of external factors or compounds on early embryo development. This is because the embryos can be easily manipulated, especially the gastrula chick embryos could be incubated in EC culture, and later chick embryos could be manipulated with the help of windowed fertilized eggs. In other word, the chick embryo model allows direct observation of the embryo development at any stage in either EC culture or narrow windowed eggshell following the experimental manipulations [34].

In the traditional medicines of many East Asian countries, the roots of *Scutellaria baicalensis* Georgi have been extensively utilized to reduce

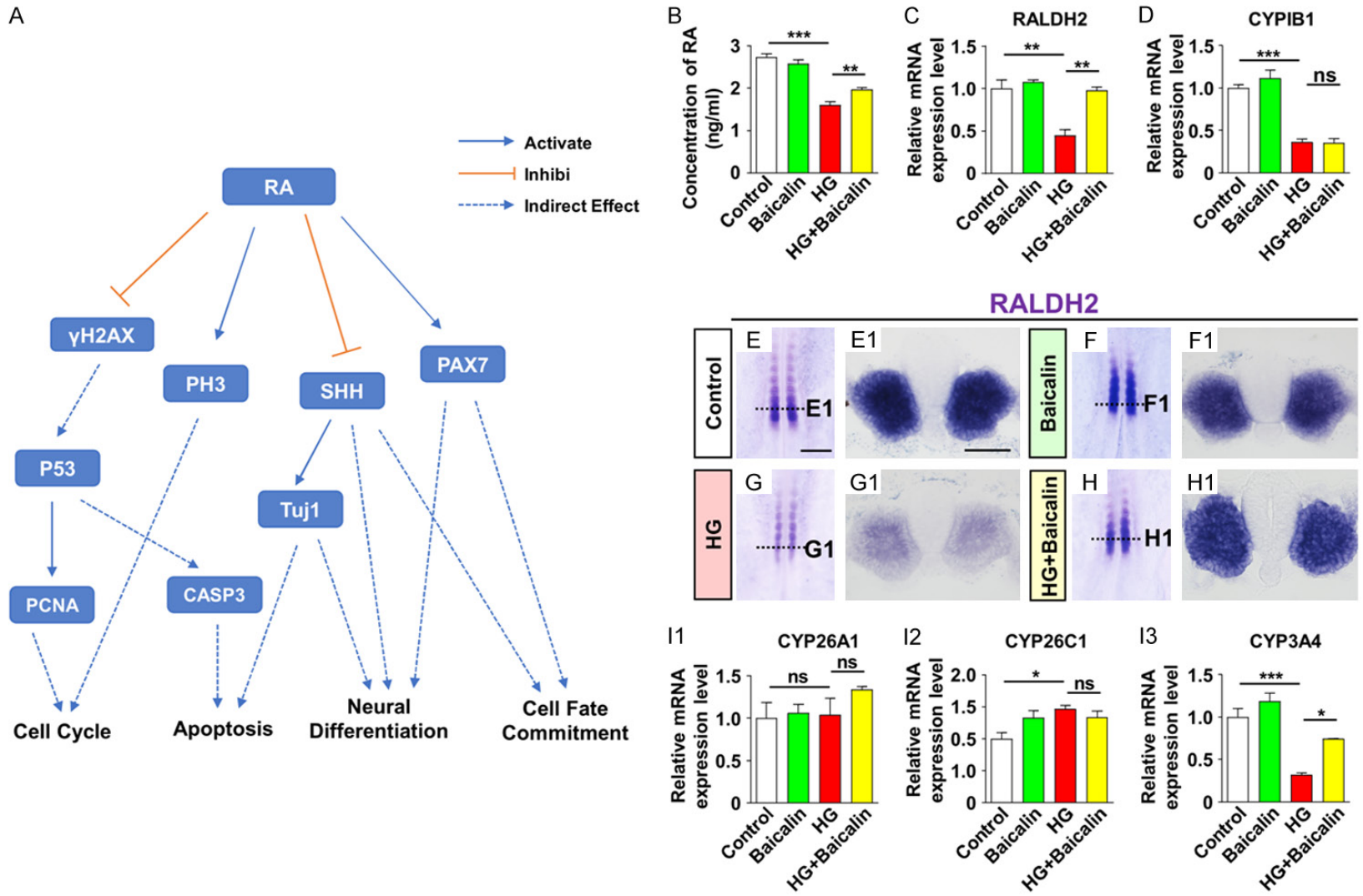

Figure 6. The assessment of RA signaling molecule expressions in gastrula chick embryos in the absence/presence of HG and Baicalin. (A) The results from the GO enrichment analysis and KEGG pathway enrichment analysis showed that the genes in our study were mainly related to cell cycle, apoptosis, neural differentiation and cell fate commitment and can be regulated by RA. (B-D, I1-I3) Bar charts showing the concentration of RA (determined using Elisa) (B), and the mRNA expression (quantitative PCR) of RALDH2 (C), CYPIB1 (D), CYP26A1 (I1), CYP26C1 (I2), CYP3A4 (I3) in HH10 chick embryo neural tubes from control, 6 μM Baicalin, 50 mM HG, 50 mM HG + 6 μM Baicalin group respectively. (E-H) The representative images of whole-mount *in situ* hybridization for RALDH2 at HH10 chick embryos from control (E), Baicalin (F), HG (G), HG + Baicalin (H) groups. (E1-H1) The transverse sections from the level indicated by dotted lines in (E-H) respectively. For (B, E-H),

n=5 in each group, for (C, D, I1-I3), n>3 in each group, relative to GAPDH mRNA level, ns, refers to no significances, *P<0.05, **P<0.01, ***P<0.001. Data were presented as mean ± SE. Statistical significances were assessed by one-way ANOVA and Turkey's multiple comparisons test. Scale bars =300 μm in (E-H); 100 μm in (E1-H1).

inflammation [35]. As a glycoside is present in *Scutellaria baicalensis* Georgi, Baicalin is metabolized to baicalein, with the action of intestinal β-glucuronidase in the intestine [36]. Once Baicalin and baicalein are absorbed in the intestine, they could be detected in blood [37]. Furthermore, accumulating evidences indicate that both Baicalin and baicalein exhibit comprehensive biological and pharmacological functions, such as anti-inflammation, anti-cancer and anti-pruritic effects [38-40], which inspired us of potentially applying Baicalin to prevent or reverse the embryo malformation induced by HG [21]. It should be noted that Baicalin could go through placental barrier and potentially impair embryos when it exists in maternal blood. Indeed, Song *et al*. reported that Baicalin could pass through placental barriers of rats in different gestational stages, indicating that the potential embryotoxicity of Baicalin should be provided with appropriate consideration when applied during pregnancy [41]. That is, if the potential embryotoxicity of Baicalin could be avoided, the applied Baicalin in pregnant women could be exposed to developing embryos. In regard to this issue, we established Baicalin (6 μM) alone group in every experiment conducted in this study and found that Baicalin itself did not have negative effects on embryo development (Supplementary Figure 1). On the contrary, Baicalin dramatically alleviated the HG-induced defects in differentiation of neural precursor cells at early neurulation and neurologic anomalies at relatively late stage of development (**Figures 1**, **2**). This finding is of significance, as the incidence of NTDs is up to 0.5-2/1000 around the world [5]. Of note, NTDs are mainly considered to be derived from the aberrant development and closure of the neural tube [4].

Proper development of neural tube stringently relies on integration of several important cellular processes, such as cell proliferation, apoptosis, and differentiation [42]. If developmental process of neural tube is disturbed by any intrinsic genetic variation or externally detrimental chemical, biological factors, NTDs could occur in neonates. In this study, we found that HG impaired neuronal differentiation as demonstrated by suppressed Tuj1 expression during early embryo development, which was potentially associated with increased incidence of NTDs (**Figures 1**, **2**). Furthermore, we observed that Baicalin administration alleviated the impaired neuronal differentiation induced by HG at neurulation stage, indicating that earlier application of Baicalin might result in enhanced treatment effect of confronting HG-interfered neural differentiation and even reducing the incidence of HG-induced risk for NTDs. Previous embryological experiments identified that the expressions of dorsal-ventral genes that are mediated by 4 signaling molecules, namely fibroblast growth factors (FGFs), retinoic acid (RA), sonic hedgehog (SHH) and bone morphogenetic proteins (BMPs) regulates neural differentiation and neural tube closure [30]. In this study, we found that Baicalin administration effectively rescued HG-suppressed cell numbers on the dorsal surface of neural tube (**Figure 3**). However, SHH, the gene expressed on ventral surface of neural tube, is only partially rescued by Baicalin (Supplementary Figure 2), indicating that Baicalin protects embryonic neurogenesis was only partially through affecting the gene expression pattern in dorsoventral neural tube.

It is well established that both apoptotic cell death and homocysteine production would be dramatically increased by hyperglycemia [43-45]. Homocysteine could induce DNA damage and P53 activation in neuron [46]. Thus, we investigated whether or not cell survival was a key link for Baicalin against poor neurogenesis induced by HG. Our results revealed that the inhibited-cell proliferation and enhanced-cell apoptosis induced by hyperglycemic condition was dramatically reversed by Baicalin administration (**Figures 4**, **5**). Meanwhile, the fact that Baicalin administration could abolish HG-induced high γH2AX expression indicates that Baicalin might target on HG-induced excessive homocysteine production and cell apoptosis derived from DNA damage, which in turn contribute to abnormal neurogenesis (**Figure 5**).

It has been reported that RA plays an important role in inducing motor neuron specification

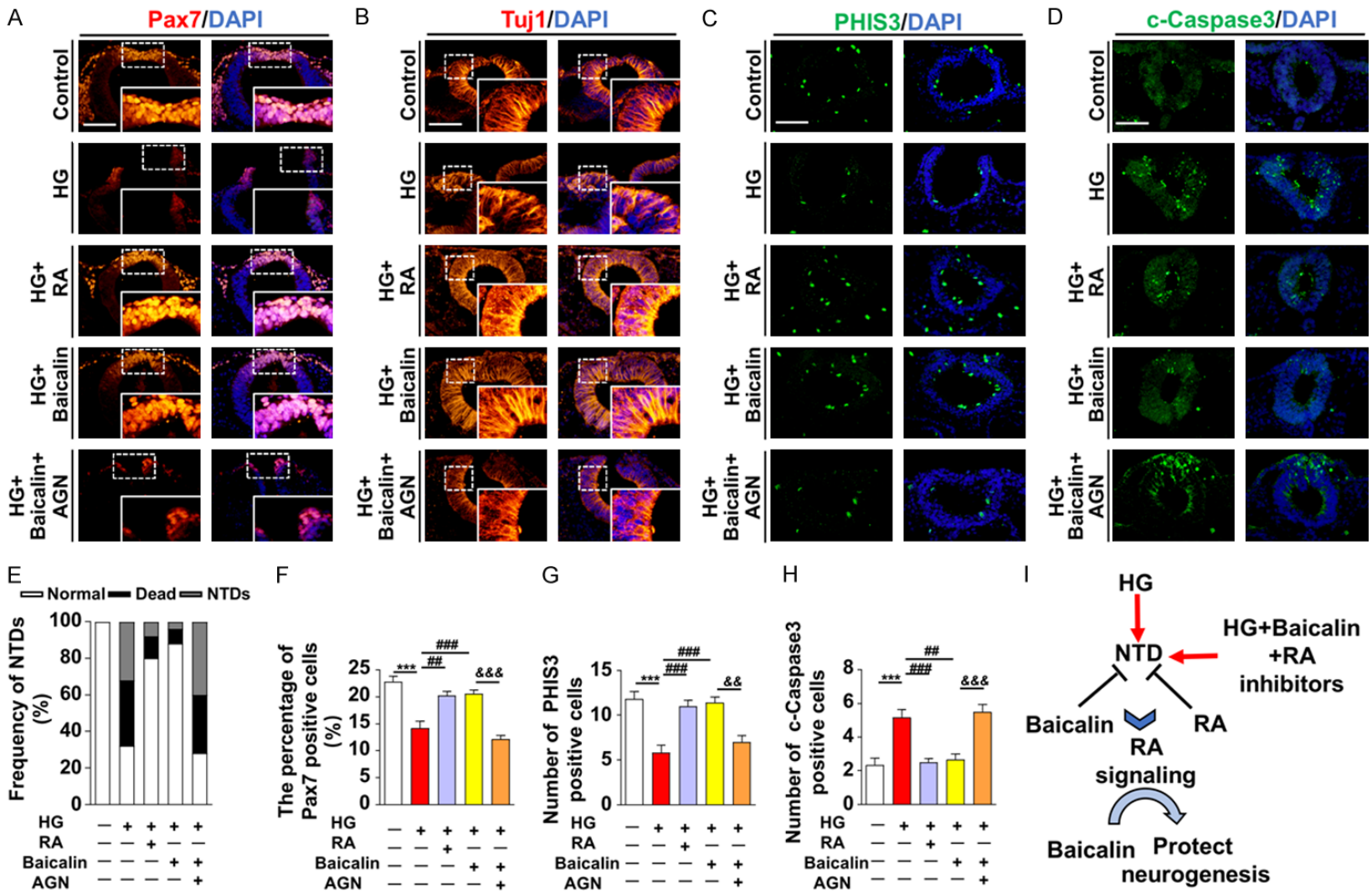

Figure 7. The assessment of NTDs characterized by neural tube development and neural differentiation following blockage of RA signaling with AGN (potent antagonist of RA receptors) in the absence/presence of HG and Baicalin. (A-D) The representative Pax7, Tuj1, PHIS3 and c-Caspase3 immunofluorescent staining of HH10 chick embryos from control, 50 mM HG, 50 mM HG + 10^{-6} M RA, 50 mM HG + 6 μM Baicalin, 50 mM HG + 6 μM Baicalin + 10^{-5} M AGN group respectively. The high magnification images are from the sites indicated by dotted squares accordingly. (E-H) Bar charts showing the comparisons of embryo NTDs incidences (E), the Pax7 positive cell percentages in the total DAPI-labelled cells of neural tubes (F), the PHIS3 positive cell percentages in the total DAPI-labelled cells of neural tubes (G) and the C-caspase3 positive cell (H) in HH10 chick embryo neural tubes from control, HG, HG + RA, HG + Baicalin, HG + Baicalin + AGN group respectively. (I)

The sketches illustrating the possible RA role on Baicalin confronts HG-induced NTDs. For (E), n=25 in each group, for (F-H), n=6 in each group, **P<0.01 and ***P<0.001 vs control; ##P<0.01 and ###P<0.001 vs HG; &&P<0.01 and &&&P<0.001 vs HG + Baicalin. Data were presented as mean ± SE. Statistical significances were assessed by one-way ANOVA and Turkey's multiple comparisons test. Scale bars =100 μm in (A-D).

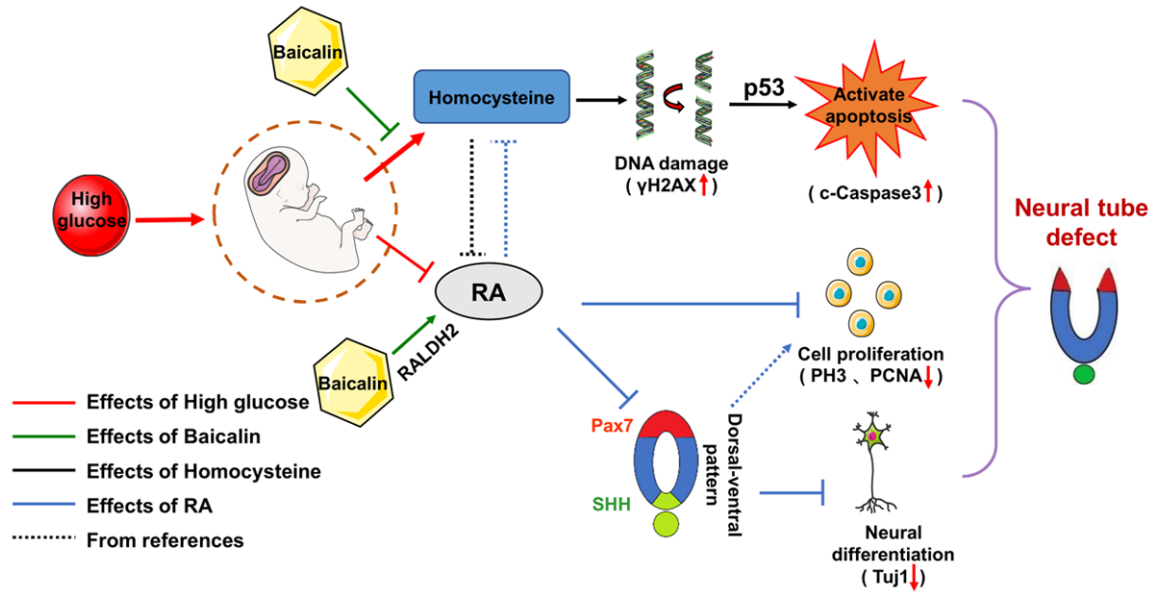

Figure 8. Model depicting how Baicalin administration improves HG-induced NTDs and abnormal neurogenesis through activation of RA signaling.

[47]. Wilson et al. also have verified the importance of RA signaling for primary neurulation in avian embryos since the lack of RA leads to neurological malformations including reducted cell proliferation and inefficient neuronal differentiation [48], suggesting that RA is an indispensable part in vertebrate neural tube morphogenesis. In this study, bioinformatics analysis suggested the alteration of RA signaling could be a decisive factor in the process of HG exposure-induced abnormal neurogenesis (**Figure 6A**). The fact that Baicalin administration altered the RA concentration confirmed the cognition obtained by bioinformatics analysis (**Figure 6B**). This might be explained that Baicalin alters the activity of RA generating enzyme through regulating the expression of RALDH2 (rather than CYP1B1), which has been identified as a major RA generating enzyme in early embryo [49, 50]. We also detected the enzymes that regulate RA clearance, such as CYP26A1, CYP26C1 and CYP3A4 [51]. Results suggested that RA clearance was not as important as RA generation during the progress when Baicalin rescued HG-induced neural tube defects. More importantly, it is well known that RA signaling is mediated through the action of retinoic acid receptors (RARs), such as RARα and RARβ, which are the members of the nuclear receptor superfamily and function as ligand-dependent transcription factors [52, 53]. Combinational knockout of RARα and RARβ leads to developmental defects and other congenital malformations [54]. In this study, the HG exposure inhibited the expressions of RARα and RARβ at mRNA level. However, the fact, which the expression of RARα instead of RARβ was significantly rescued by Baicalin administration, suggested that RA signaling play a vital role on the protective effect of Baicalin via RARα. At last, we revealed HG-induced neural tube malformation could be rescued by RA activation, which serves as an active participator in regulating neuronal differentiation and the survival of neural precursor cells. This also could explain why the blockage of RA-mediated signaling could abolish the rescue effects of Baicalin on HG-induced abnormal neurulation (**Figure 7**).

Conclusion

In summary (**Figure 8**), administration of Baicalin in early chicken embryos can partially

counteract HG-induced abnormal neurodevelopment. At the same time, RA signaling works as the vital component in the process of how Baicalin rescues HG-induced abnormal neurulation, protecting the neurodevelopment of neural tube caused by HG-induced damage. By affecting the expression of the key genes in the dorsoventral side of neural tube, Baicalin exerts protective effect on neurogenesis by participating in the regulations of various cellular events, such as cell proliferation, differentiation, apoptosis, and DNA repair. Thus, administration of Baicalin may effectively reduce embryonic NTDs induced by HG, and Baicalin may be a potential drug candidate for women with gestational diabetes. There is no doubt that further precise exploration for relevant molecular mechanisms about the protective effects of Baicalin is still required.

Acknowledgements

We would like to thank Mr. Xin Luo for technical help. This study was supported by NSFC grant (31971108, 31771331, 81741016), Science and Technology Planning Project of Guangdong Province (2017A020214015, 2016B030229-002, 2017A050506029), Science and Technology Program of Guangzhou (201710010054), Special Funds for the Cultivation of Guangdong College Students' Scientific and Technological Innovation (pdjh2020a0063).

Disclosure of conflict of interest

None.

Address correspondence to: Xuesong Yang, Division of Histology and Embryology, International Joint Laboratory for Embryonic Development & Prenatal Medicine, Medical College, Jinan University, Guangzhou 510632, China. Tel: +86-20-85228316; E-mail: yang_xuesong@126.com

References

[1] Wilson L and Maden M. The mechanisms of dorsoventral patterning in the vertebrate neural tube. Dev Biol 2005; 282: 1-13.

[2] Cearns MD, Escuin S, Alexandre P, Greene ND and Copp AJ. Microtubules, polarity and vertebrate neural tube morphogenesis. J Anat 2016; 229: 63-74.

[3] Cayuso J and Marti E. Morphogens in motion: growth control of the neural tube. J Neurobiol 2005; 64: 376-387.

[4] Copp AJ and Greene ND. Genetics and development of neural tube defects. J Pathol 2010; 220: 217-230.

[5] Mitchell LE. Epidemiology of neural tube defects. Am J Med Genet C Semin Med Genet 2005; 135c: 88-94.

[6] Copp AJ, Stanier P and Greene ND. Neural tube defects: recent advances, unsolved questions, and controversies. Lancet Neurol 2013; 12: 799-810.

[7] Ejdesjo A, Wentzel P and Eriksson UJ. Influence of maternal metabolism and parental genetics on fetal maldevelopment in diabetic rat pregnancy. Am J Physiol Endocrinol Metab 2012; 302: E1198-1209.

[8] Wang XY, Li S, Wang G, Ma ZL, Chuai M, Cao L and Yang X. High glucose environment inhibits cranial neural crest survival by activating excessive autophagy in the chick embryo. Sci Rep 2015; 5: 18321.

[9] Wang G, Huang WQ, Cui SD, Li S, Wang XY, Li Y, Chuai M, Cao L, Li JC, Lu DX and Yang X. Autophagy is involved in high glucose-induced heart tube malformation. Cell Cycle 2015; 14: 772-783.

[10] Chen Y, Wang G, Ma ZL, Li Y, Wang XY, Cheng X, Chuai M, Tang SZ, Lee KK and Yang X. Adverse effects of high glucose levels on somite and limb development in avian embryos. Food Chem Toxicol 2014; 71: 1-9.

[11] Liu S, Yuan Q, Zhao S, Wang J, Guo Y, Wang F, Zhang Y, Liu Q, Zhang S, Ling EA and Hao A. High glucose induces apoptosis in embryonic neural progenitor cells by a pathway involving protein PKCdelta. Cell Signal 2011; 23: 1366-1374.

[12] Summaries for patients. Screening for gestational diabetes during pregnancy: recommendation from the U.S. preventive services task force. Ann Intern Med 2008; 148: I60.

[13] Abel EL. Prenatal effects of alcohol. Drug Alcohol Depend 1984; 14: 1-10.

[14] Wang P, Cao Y, Yu J, Liu R, Bai B, Qi H, Zhang Q, Guo W, Zhu H and Qu L. Baicalin alleviates ischemia-induced memory impairment by inhibiting the phosphorylation of CaMKII in hippocampus. Brain Res 2016; 1642: 95-103.

[15] Wang CZ, Zhang CF, Chen L, Anderson S, Lu F and Yuan CS. Colon cancer chemopreventive effects of baicalein, an active enteric microbiome metabolite from baicalin. Int J Oncol 2015; 47: 1749-1758.

[16] Wang F, Xu Z, Ren L, Tsang SY and Xue H. GABA A receptor subtype selectivity underlying selective anxiolytic effect of baicalin. Neuropharmacology 2008; 55: 1231-1237.

[17] Baek JS, Hwang CJ, Jung HW, Park YK, Kim YH, Kang JS and Cho CW. Comparative pharmacokinetics of a marker compound, baicalin in

KOB extract after oral administration to normal and allergic-induced rats. Drug Deliv 2014; 21: 453-458.
[18] Zhang YM, Zhang YY, Bulbul A, Shan X, Wang XQ and Yan Q. Baicalin promotes embryo adhesion and implantation by upregulating fucosyltransferase IV (FUT4) via Wnt/beta-catenin signaling pathway. FEBS Lett 2015; 589: 1225-1233.
[19] Yin F, Liu J, Ji X, Wang Y, Zidichouski J and Zhang J. Baicalin prevents the production of hydrogen peroxide and oxidative stress induced by Abeta aggregation in SH-SY5Y cells. Neurosci Lett 2011; 492: 76-79.
[20] Qi X, Li H, Cong X, Wang X, Jiang Z, Cao R and Tian W. Baicalin increases developmental competence of mouse embryos in vitro by inhibiting cellular apoptosis and modulating HSP70 and DNMT expression. J Reprod Dev 2016; 62: 561-569.
[21] Wang G, Liang J, Gao LR, Si ZP, Zhang XT, Liang G, Yan Y, Li K, Cheng X, Bao Y, Chuai M, Chen LG, Lu DX and Yang X. Baicalin administration attenuates hyperglycemia-induced malformation of cardiovascular system. Cell Death Dis 2018; 9: 234.
[22] Jin YM, Zhao SZ, Zhang ZL, Chen Y, Cheng X, Chuai M, Liu GS, Lee KK and Yang X. High glucose level induces cardiovascular dysplasia during early embryo development. Exp Clin Endocrinol Diabetes 2013; 121: 448-454.
[23] Hamburger V and Hamilton HL. A series of normal stages in the development of the chick embryo. 1951. Dev Dyn 1992; 195: 231-272.
[24] Bayha E, Jorgensen MC, Serup P and Grapin-Botton A. Retinoic acid signaling organizes endodermal organ specification along the entire antero-posterior axis. PLoS One 2009; 4: e5845.
[25] Johnson AT, Wang L, Gillett SJ and Chandraratna RA. High affinity retinoic acid receptor antagonists: analogs of AGN 193109. Bioorg Med Chem Lett 1999; 9: 573-576.
[26] Chapman SC, Collignon J, Schoenwolf GC and Lumsden A. Improved method for chick whole-embryo culture using a filter paper carrier. Dev Dyn 2001; 220: 284-289.
[27] Henrique D, Adam J, Myat A, Chitnis A, Lewis J and Ish-Horowicz D. Expression of a delta homologue in prospective neurons in the chick. Nature 1995; 375: 787-790.
[28] Maroto M, Reshef R, Munsterberg AE, Koester S, Goulding M and Lassar AB. Ectopic Pax-3 activates MyoD and Myf-5 expression in embryonic mesoderm and neural tissue. Cell 1997; 89: 139-148.
[29] Dugaiczyk A, Haron JA, Stone EM, Dennison OE, Rothblum KN and Schwartz RJ. Cloning and sequencing of a deoxyribonucleic acid copy of glyceraldehyde-3-phosphate dehydrogenase messenger ribonucleic acid isolated from chicken muscle. Biochemistry 1983; 22: 1605-1613.
[30] Si ZP, Wang G, Han SS, Jin Y, Hu YX, He MY, Brand-Saberi B, Yang X and Liu GS. CNTF and Nrf2 are coordinately involved in regulating self-renewal and differentiation of neural stem cell during embryonic development. iScience 2019; 19: 303-315.
[31] Simon-Delso N, Amaral-Rogers V, Belzunces LP, Bonmatin JM, Chagnon M, Downs C, Furlan L, Gibbons DW, Giorio C, Girolami V, Goulson D, Kreutzweiser DP, Krupke CH, Liess M, Long E, McField M, Mineau P, Mitchell EA, Morrissey CA, Noome DA, Pisa L, Settele J, Stark JD, Tapparo A, Van Dyck H, Van Praagh J, Van der Sluijs JP, Whitehorn PR and Wiemers M. Systemic insecticides (neonicotinoids and fipronil): trends, uses, mode of action and metabolites. Environ Sci Pollut Res Int 2015; 22: 5-34.
[32] He YQ, Li Y, Wang XY, He XD, Jun L, Chuai M, Lee KK, Wang J, Wang LJ and Yang X. Dimethyl phenyl piperazine iodide (DMPP) induces glioma regression by inhibiting angiogenesis. Exp Cell Res 2014; 320: 354-364.
[33] Jin Y, Wang G, Han SS, He MY, Cheng X, Ma ZL, Wu X, Yang X and Liu GS. Effects of oxidative stress on hyperglycaemia-induced brain malformations in a diabetes mouse model. Exp Cell Res 2016; 347: 201-211.
[34] Tufan AC and Satiroglu-Tufan NL. The chick embryo chorioallantoic membrane as a model system for the study of tumor angiogenesis, invasion and development of anti-angiogenic agents. Curr Cancer Drug Targets 2005; 5: 249-266.
[35] Ishimaru K, Nishikawa K, Omoto T, Asai I, Yoshihira K and Shimomura K. Two flavone 2'-glucosides from Scutellaria baicalensis. Phytochemistry 1995; 40: 279-281.
[36] Noh K, Kang Y, Nepal MR, Jeong KS, Oh do G, Kang MJ, Lee S, Kang W, Jeong HG and Jeong TC. Role of intestinal microbiota in baicalin-induced drug interaction and its pharmacokinetics. Molecules 2016; 21: 337.
[37] Kang MJ, Ko GS, Oh DG, Kim JS, Noh K, Kang W, Yoon WK, Kim HC, Jeong HG and Jeong TC. Role of metabolism by intestinal microbiota in pharmacokinetics of oral baicalin. Arch Pharm Res 2014; 37: 371-378.
[38] Lin CC and Shieh DE. The anti-inflammatory activity of Scutellaria rivularis extracts and its active components, baicalin, baicalein and wogonin. Am J Chin Med 1996; 24: 31-36.
[39] Li-Weber M. New therapeutic aspects of flavones: the anticancer properties of Scutellaria and its main active constituents Wogonin, Baicalein and Baicalin. Cancer Treat Rev 2009; 35: 57-68.

[40] Trinh HT, Joh EH, Kwak HY, Baek NI and Kim DH. Anti-pruritic effect of baicalin and its metabolites, baicalein and oroxylin A, in mice. Acta Pharmacol Sin 2010; 31: 718-724.
[41] Song D, Guo J, Wang Y, Pan G, Li P, Zhang W and Song H. Ingredients of Shuanghuanglian injection powder permeation through placental barrier of rat in pregnancy. Zhongguo Zhong Yao Za Zhi 2010; 35: 1626-1629.
[42] Stevenson RE, Seaver LH, Collins JS and Dean JH. Neural tube defects and associated anomalies in South Carolina. Birth Defects Res A Clin Mol Teratol 2004; 70: 554-558.
[43] Haribalaganesh R, Sheikpranbabu S, Elayappan B, Venkataraman D and Gurunathan S. Pigment-epithelium-derived factor down regulates hyperglycemia-induced apoptosis via PI3K/Akt activation in goat retinal pericytes. Angiogenesis 2009; 12: 381-389.
[44] Han SS, Wang G, Jin Y, Ma ZL, Jia WJ, Wu X, Wang XY, He MY, Cheng X, Li WJ, Yang X and Liu GS. Investigating the mechanism of hyperglycemia-induced fetal cardiac hypertrophy. PLoS One 2015; 10: e0139141.
[45] Seghieri G, Breschi MC, Anichini R, De Bellis A, Alviggi L, Maida I and Franconi F. Serum homocysteine levels are increased in women with gestational diabetes mellitus. Metabolism 2003; 52: 720-723.
[46] Kruman II, Culmsee C, Chan SL, Kruman Y, Guo Z, Penix L and Mattson MP. Homocysteine elicits a DNA damage response in neurons that promotes apoptosis and hypersensitivity to excitotoxicity. J Neurosci 2000; 20: 6920-6926.
[47] Novitch BG, Wichterle H, Jessell TM and Sockanathan S. A requirement for retinoic acid-mediated transcriptional activation in ventral neural patterning and motor neuron specification. Neuron 2003; 40: 81-95.
[48] Wilson L, Gale E and Maden M. The role of retinoic acid in the morphogenesis of the neural tube. J Anat 2003; 203: 357-368.
[49] Niederreither K, McCaffery P, Drager UC, Chambon P and Dolle P. Restricted expression and retinoic acid-induced downregulation of the retinaldehyde dehydrogenase type 2 (RALDH-2) gene during mouse development. Mech Dev 1997; 62: 67-78.
[50] Williams AL, Eason J, Chawla B and Bohnsack BL. Cyp1b1 regulates ocular fissure closure through a retinoic acid-independent pathway. Invest Ophthalmol Vis Sci 2017; 58: 1084-1097.
[51] Ross AC and Zolfaghari R. Cytochrome P450s in the regulation of cellular retinoic acid metabolism. Annu Rev Nutr 2011; 31: 65-87.
[52] Chen J and Li Q. Implication of retinoic acid receptor selective signaling in myogenic differentiation. Sci Rep 2016; 6: 18856.
[53] Gutierrez-Mazariegos J, Schubert M and Laudet V. Evolution of retinoic acid receptors and retinoic acid signaling. Subcell Biochem 2014; 70: 55-73.
[54] Huang P, Chandra V and Rastinejad F. Retinoic acid actions through mammalian nuclear receptors. Chem Rev 2014; 114: 233-254.

Supplementary Table 1. Primers sequence for qPCR

Genes	Forward (5'-3')	Reverse (3'-5')
Tuj1(c)	ATGAGCATGGCATAGACCCC	GGCACGTACTTGTGAGAGGAG
P53(c)	TGCTGAACCCCGACAATGAG	GTCAGTCCGAGCCTTTTTGC
c-Caspase3(c)	TGGTGGAGGTGGAGGAGC	TGTCTGTCATCATGGCTCTTG
γH2AX(c)	AGGCATCTTCTCTTCGTCGC	AGGAACGAGACTTGGCCTTC
RALDH2(c)	ATTCCTGCAAGCCTTCTACG	TTGCTCCTTCAGTAATGCCG
CYPIB1(c)	CCTCATCAGGTATCCAAAAGTGC	AAAGCCACGATGTAGGGCAA
CYP26A1(c)	ACCGCAAAAAGGTGATCATGC	TTCACCTCGGGATACACCAG
CYP3A4(c)	GAGCAAGGGAGCAAACAAGAC	TCTTGAAGGTCTGGTAGGGC
SHH(c)	CCATCACTCCGAGGAATCGC	CCCAGCACATAGACACGTTG
RARα(c)	TGTCTAGTGAGGGGCACCA	TCCGTCCTTTGGTTAAGCGG
RARβ(c)	ATTCATGATTCGGGGCTGGG	GCGCTCTGCAAAAGTGCTTA
GAPDH(c)	TCAAATGGGCAGATGCAGGT	AGCTGAGGGAGCTGAGATGA

Notes: "c" genes from chicken.

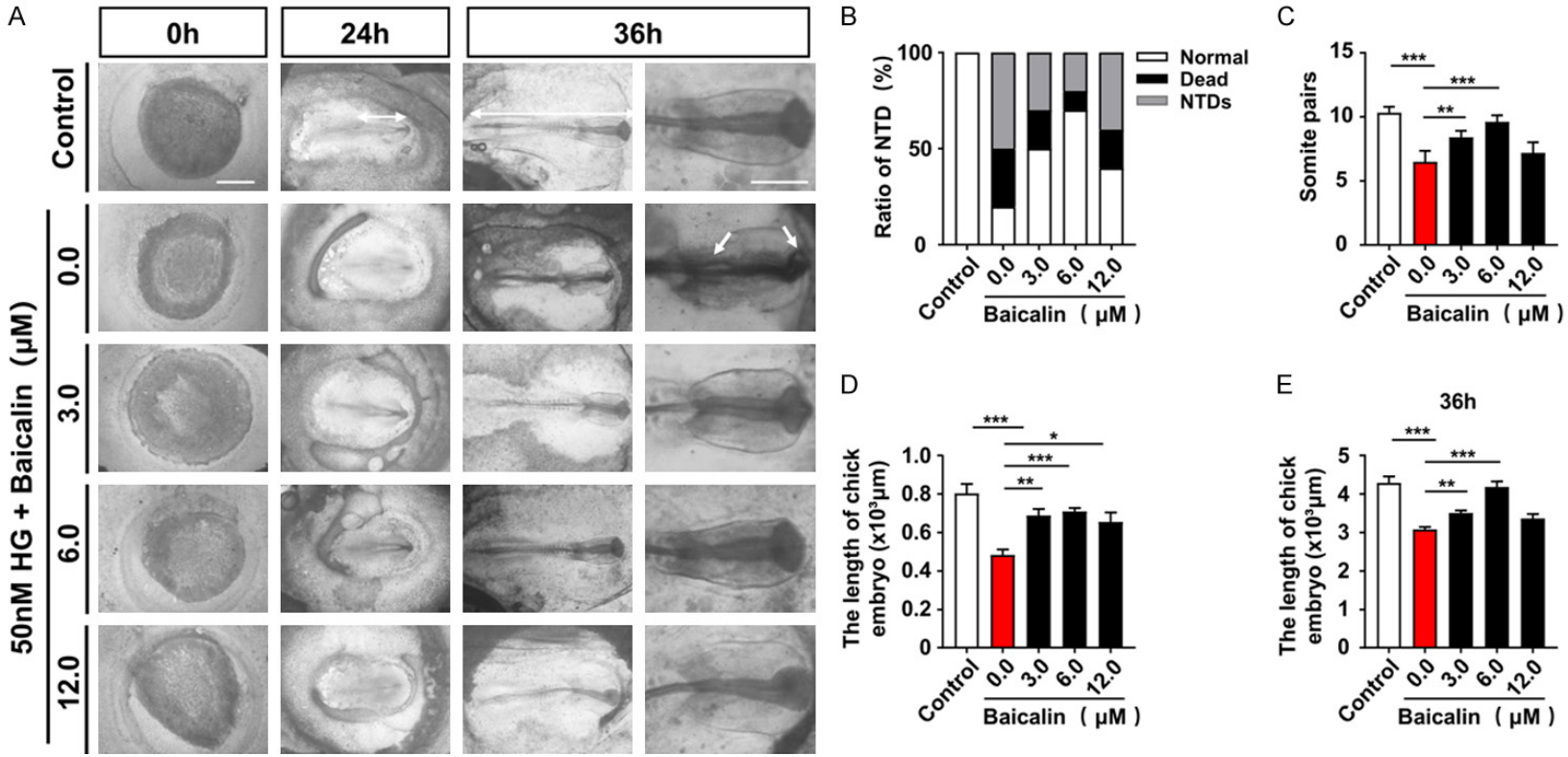

Supplementary Figure 1. The assessment of the development of gastrula chick embryos in the absence/presence of HG and Baicalin. (A) The representative bright-field gastrula chick embryos incubated for 0, 24, 36 hours in absence/presence of 50 mM HG and different concentrations (0, 3, 6 12 μM) of Baicalin. (B-E) Bar charts showing the comparisons of NTDs incidences (%) (B), number of pairs of somites (C), the lengths of chick embryos at 24-hour (D) and 36-hour (E) incubation among the control, HG and different concentrations of Baicalin groups. For (A, B), n=30 in each group, for (C-E), n=10 in each group, *P<0.05, **P<0.01, ***P<0.001. Data were presented as mean ± SE. Statistical significances were assessed by one-way ANOVA and Turkey's multiple comparisons test. Scale bars =500 μm in (A).

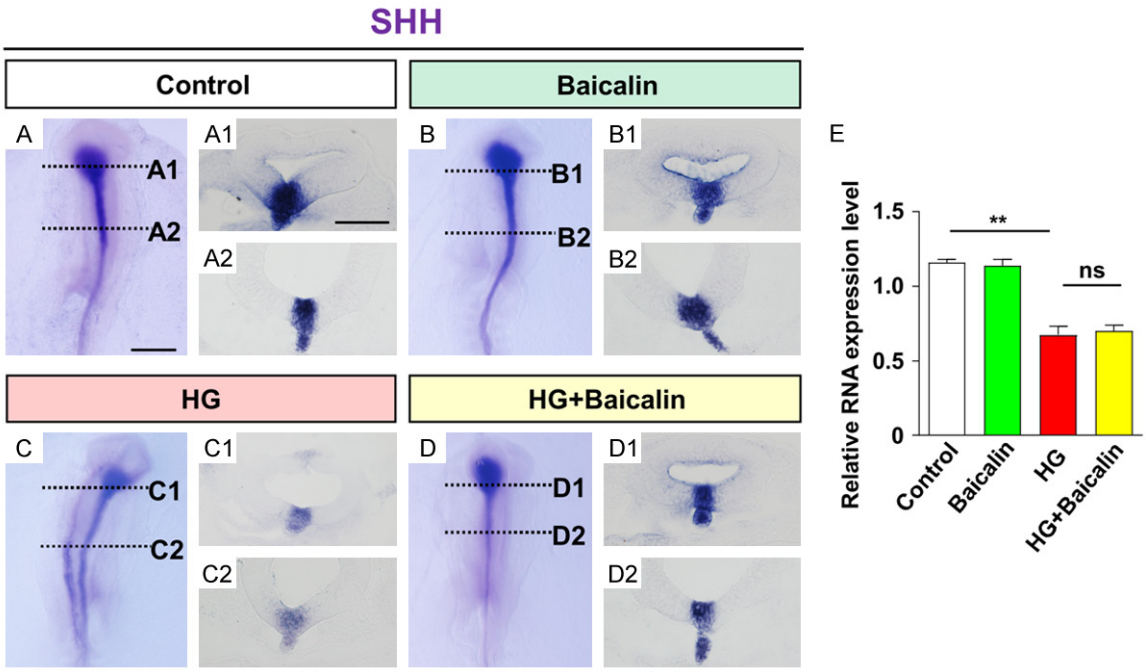

Supplementary Figure 2. The assessment of the expressions of SHH in the absence/presence of HG and Baicalin. (A-D) The representative images of whole-mount *in situ* hybridization for SHH at HH10 chick embryos from control (A), Baicalin (B), HG (C), HG + Baicalin (D) groups. (A1-D1, A2-D2) The transverse sections from the levels indicated by dotted lines in (A-D) respectively. (E) The bar chart showing the mRNA expressions (quantitative PCR) of SHH in HH10 chick embryos among control, Baicalin, HG, HG + Baicalin groups. For (A-D), n=6 in each group, for (E), n>3 in each group, relative to GAPDH mRNA level, ns, refers to no significances, **P<0.01. Data were presented as mean ± SE. Statistical significances were assessed by one-way ANOVA and Turkey's multiple comparisons test. Scale bars =300 μm in (A-D); 100 μm in (A1-D1, A2-D2).

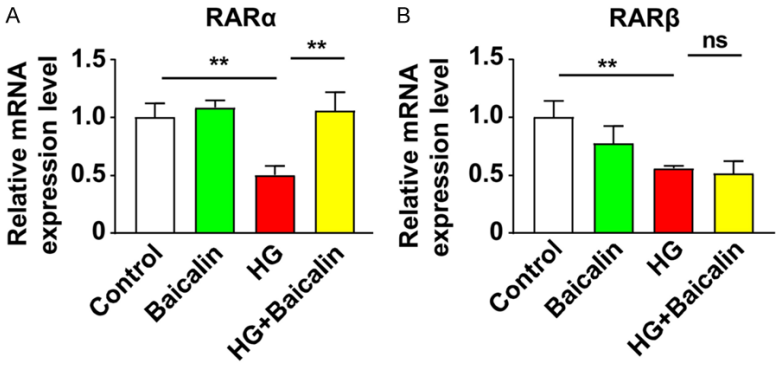

Supplementary Figure 3. The assessment of the expressions of RA receptors in the absence/presence of HG and Baicalin. A, B. The bar charts showing the data of quantitative PCR about the expressions of RARα and RARβ at mRNA level in HH10 chick embryos among control, Baicalin, HG, HG + Baicalin groups. n>3 in each group, relative to GAPDH mRNA level. ns, refers to no significances, **P<0.01. Data were presented as mean ± SE. Statistical significances were assessed by one-way ANOVA and Turkey's multiple comparisons test.